Analytical Methods

Accepted Manuscript

This article can be cited before page numbers have been issued, to do this please use: X. He, H. Han, W. Shi, J. Dong, X. Lu, W. Yang and X. Lu, *Anal. Methods*, 2020, DOI: 10.1039/D0AY00025F.

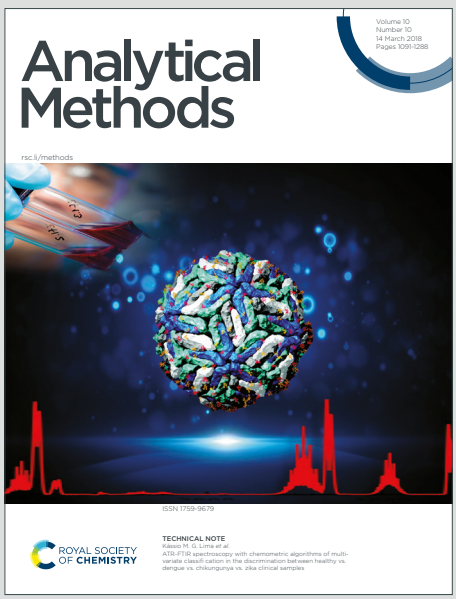

ROYAL SOCIETY OF CHEMISTRY

rsc.li/methods

View Article Online
DOI: 10.1039/D0AY00025F

Label-free electrochemical DNA biosensor for kanamycin detection based on diblock DNA with poly-cytosine as high affinity anchors on graphene oxide

Xiaoyan He*, Huimin Han, Wenyu Shi, Jiandi Dong, Xiong Lu, Wu Yang, Xiaoquan Lu

Key Laboratory of Bioelectrochemistry and Environmental Analysis of Gansu, College of Chemistry and Chemical Engineering, Northwest Normal University, Lanzhou 730070, P. R. China

*Corresponding Author：

Xiaoyan He：hexy09@163.com

Tel：+86-13919132753

Abstract

It is urgent to develop a more simple and sensitive method to detect antibiotic residues considering the harm of antibiotic residues in food to human body. Herein we designed a label-free electrochemical DNA biosensor for sensitive detection of kanamycin (KAN) based on diblock DNA with 15-mer of poly-cytosine (poly-C). The diblock DNA can be immobilized to graphene oxide (GO) due to strong physical adsorption between the 15-mer of poly-C and GO. The aptamer of KAN acted as the other block used for rapidly binding the target. It can specifically capture the target, which leads to the change of electrochemical signal. Consequently, the DNA

View Article Online
DOI: 10.1039/D0AY00025F

biosensor exhibited high sensitivity and specificity towards KAN, the linear range was from 0.05 pM to 100 nM with a detection limit of 0.0476 pM. The developed DNA biosensor was constructed easily and showed promising applications for the detection of antibiotic residues in food safety.

Keywords

electrochemical DNA biosensor; poly-cytosine; graphene oxide; adsorption; kanamycin

1. Introduction

Kanamycin is one of the aminoglycoside antibiotics and has strong bactericidal effect.[1] It was used in the treatment of some animal diseases frequently.[2] If kanamycin were overused, the residues will be inevitable in foods of animal origin,[3] such as milk and pork. However, the accumulation of kanamycin in the body through food can cause many diseases to harm consumer's healthy, such as toxicity to the kidney and hearing loss.[4-6] In order to prevent something unfortunate from happening, it is extremely urgent to develop a more simple, rapid and sensitive method to detect kanamycin residues in food.

Up to now, many techniques have been developed to detect kanamycin. Typical traditional detection methods include high performance liquid chromatograph (HPLC) analysis,[7] fluorescence method and colorimetric analysis and so on.[8-10] Each of these approaches has obvious drawback, such as the expensive equipment of HPLC, the complexity of the fluorescence and the time-consuming of the colorimetric method. Moreover, the detection results of these conventional methods were often not

View Article Online
DOI: 10.1039/D0AY00025F

satisfactory. Compared to the traditional detection ways, immunoassay techniques are more sensitive and efficient. Wei's group have been developed a label-free electrochemical immunosensor.[11] Although the method achieved relatively good detection of kanamycin, it still showed weak specificity due to cross-reactivity from similar molecules. Furthermore, if the antibodies acted as biorecognition probe, high production cost was also an important drawback.[12]

In the later research on the detection method of antibiotics, the aptamer has attracted great attention. Aptamers are single strands of specific DNA or RNA obtained through in vitro screening, which has the advantages of easy manipulation, high stability, small size and easy modification.[13,14] In addition, the aptamer has higher specificity and selectivity than the antibody or antigen, it can quickly and accurately identify the target.[15] It is essential to achieve simple, efficient, and strong binding of aptamers or other DNA sequence for the successful construction of DNA biosensor. Most of reports have used DNA strands modified by functional group for covalent binding to achieve the immobilization, such as DNA sequences modified with thiol or amino to facilitate covalent bonding with the gold or carboxyl-modified surface.[16-18] Jayakumar's group has applied the Au-S covalent bond between gold nanoparticles and thiol-modified single strand DNA (ssDNA) to immobilize the capture ssDNA.[19] Miodek and his colleagues have modified DNA probe onto the biosensor via covalent link between the ferrocene functionalized with activated carboxylic groups and a amino on 5'-end position of the DNA probe.[20] Moreover, the avidin-biotin interaction and ferrocene marker were used for improving the sensitivity

View Article Online
DOI: 10.1039/D0AY00025F

of the DNA biosensor.[21,22] Nevertheless, these sensors have always been limited by the defect of costly and time-consuming.

However, covalent immobilization cannot avoid the shortcomings with the modification of DNA sequences by functional group, and have the risk of damaging the activity of DNA sequences in different level.[23] In view of keeping the activity of the DNA sequence, the non-covalent bond is more beneficial than covalent binding. In recent years, as the rapid development of DNA-functionalized nanomaterials, it has significant application prospect in biosensors and other fields.[24,25] As typical nanomaterials, graphene oxide (GO) have favorable stability and unique physical and chemical properties,[26] and it can conjugate with DNA via non-covalent bond (physical adsorption) due to characteristic structure. In order to improve adsorption, Huang and his partners found that poly-cytosine (poly-C) DNA can adsorb well with GO.[27] Considering various factors, poly-C DNA and GO achieved the best adsorption effect and the 15-mer was the optimal length for the diblock DNA with poly-C.[28] 15-mer of poly-C of the diblock DNA can be acted as anchor on the surface of GO and the other DNA block can be used to hybridize, therefore, diblock DNA can be applied to the design of DNA biosensor completely.

Moreover, nanomaterials played a very important part in amplifying the signal of the biosensor,[29-32] for example, gold nanoparticles and carbon nanotubes. Multi-walled carbon nanotubes (MWCNTs) can provide a large ratio of surface-to-volume, chemical and thermal stability, and have the property of fast electron transfer.[33-35] Giving the findings, we have designed a DNA biosensor based

View Article Online
DOI: 10.1039/D0AY00025F

on the diblock DNA with poly-C as the anchor for sensitive detection of kanamycin. In this work, MWCNTs played a role in amplifying the electrochemical signal and were acidified firstly for better dispersion. In addition, the designed diblock DNA include optimal 15-mer of poly-C and the other block, aptamer of kanamycin. Hence, the diblock DNA was used not only for adsorption with GO but also for hybridization with the target. The results indicated that we have achieved the sensitive and efficient detection toward the kanamycin. It's worth noting that our approach was very simple compared to many other techniques.

2. Experimental

2.1 Reagents

Kanamycin (KAN, 94%), chloramphenicol (CAP, 98%), amoxicillin (AMX, 98%), 4-(2-hydroxyethyl) piperazine-1-ethanesulfonate (HEPES) and chitosan were purchased from Aladdin Reagents Co., Ltd. (Shanghai, China). Streptomycin (STR, 99%), bovine serum albumin (BSA, 98%) and oxytetracycline (OTC, 930U/mg) were provided by Shanghai Yuanye Biological Technology Co., Ltd. (Shanghai, China). The DNA sequence of 5′-TGGGGGTTGAGGCTAAGCCGACCCCCCCCCCCCCC-3′ was prepared by Shanghai Sangon Biotechnology Co., Ltd. Graphene oxide (GO) dispersion (5mg/mL) was supplied by Carbonium Graphite Technology Co., Ltd. (Suzhou, China). Tris (hydroxymethyl) methyl aminomethane (Tris) was purchased from Shanghai Zhongqin Chemical Reagent Co., Ltd. Multi-walled carbon nanotubes (MWCNTs) (20-40 nm) were provided by Shenzhen Nanotech Port Co., Ltd. (Shenzhen, China).

View Article Online
DOI: 10.1039/D0AY00025F

Fresh milk was purchased from a local supermarket. All other chemicals used in this paper were of analytical grade.

2.2 Apparatus

The electrochemical experiments were performed by an electrochemical workstation (CHI660E, Shanghai Chenhua Instrument Co. Ltd, China) at room temperature. The glassy carbon electrode (GCE) acted as work electrode, the saturated calomel electrode and a platinum wire were served as the reference electrode and auxiliary electrode respectively. In addition, the morphology of the surface of electrodes was monitored by a scanning electron microscope (SEM, Quanta 200, philips-FEI).

2.3 Acidification of MWCNTs

0.5 g of MWCNTs were added to a 250 mL flask, then add 100 ml mixture of concentrated sulfuric acid and concentrated nitric acid to the flask with a volume ratio of 3:1. Subsequently, the flask was heated with stirring at 60 ℃ for 8 h. And we used 0.22 μm polytetrafluoroethylene microfiltration membrane for filtration and washed with deionized water until the filtrate was neutral. MWCNTs were dried at 80 ℃ after filtration and ground to fine powder. Finally, MWCNTs were ultrasonically dispersed for 40 min in 1% chitosan solution to a final concentration of 2 mg/mL.

2.4 Preparation of poly-C DNA/GO adsorption complex[28]

First of all, the poly-C DNA was diluted with Tri-HCl (pH=8.0) to 100 μM. Typically, the poly-C DNA and GO were mixed in the buffer, which was consist of 150 mM NaCl, 1 mM $MgCl_2$, 25 mM HEPES (pH =7.5). The final volume of the

View Article Online
DOI: 10.1039/D0AY00025F

mixture was 500 μL, and the final concentration of poly-C DNA and GO was 10 μM and 1 mg/mL respectively. Next, the poly-C DNA/GO sample was incubated at room temperature for one night. The conjugate of poly-C DNA and GO were washed 3 times with the above buffer under 8000 rpm for 6 min, finally, the product was stored at 4 ℃ until it was used.

2.5 Fabrication of the DNA biosensor

Consistent with the previous methods of treating electrodes, we polished the GCE with 0.3 mm alumina slurry on the chamois firstly. Then the GCE was ultrasonic washed with the mixture of absolute ethanol and deionized water for 5 min, and ultrasonic washed with deionized water for 5 min again. Next, the high purity nitrogen was used for drying the GCE. 10 μL of the dispersions of MWCNTs was dropped on the surface of the GCE, and dried at room temperature. Then 10 μL of the poly-C DNA/GO adsorption complex was dipped on the MWCNTs/GCE for overnight to dry at 4 ℃. Finally, the 10 μL of 1% BSA was dropped on the poly-C DNA/GO/MWCNTs/GCE and incubated for 1 h. The designed DNA biosensor was named BSA/poly-C DNA/GO/MWCNTs/GCE. Meanwhile, we have also monitored the process of constructing the DNA biosensor by cyclic voltammetry (CV) and electrochemical impedance spectroscopy (EIS) in PBS (0.2 M, pH=7.4) solution containing 5.0 mM $[Fe(CN)_6]^{3-/4-}$ and 0.1 M KCl.

2.6 Detection of KAN with the DNA biosensor

The differential pulse voltammetry (DPV) was conducted toward KAN in the PBS (0.2 M, pH=7.4) solution containing 5.0 mM $[Fe(CN)_6]^{3-/4-}$ and 0.1 M KCl, and the

View Article Online
DOI: 10.1039/D0AY00025F

$[Fe(CN)_6]^{3-/4-}$ acted as redox probe. The measurement of DPV was carried out from -0.1 V - 0.4 V, and the pulse amplitude was 50 mV with the pulse period of 50 ms.

3. Results and discussion

3.1 Mechanism of the DNA biosensor

In this work, the electrochemical DNA biosensor was simply constructed based on the diblock DNA with 15-mer of poly-C. It can be seen in Scheme 1, as a high-affinity ligand of GO, the poly-C can interact with GO due to the π–π stacking and carboxyl groups between them.[27] Furthermore, according to the research, the 15-mer of poly-C can efficiently resist the displacement of other interference. The DNA sequence was designed to be double-block, one block was acted as an anchor to absorb the GO, and the other was consisting of the aptamer of KAN. In this way, GO was considered as a special nanomaterial of DNA-functionalized for the detection of KAN. In order to achieve the high sensitivity during the sensing process, MWCNTs was modified on the GCE firstly.[36] When the target KAN appeared, the electrochemical signal changed significantly with the specific binding of KAN and aptamer. Above all, label-free electrochemical DNA biosensor was simply fabricated and used for the sensitive detection of KAN.

3.2 SEM characterization of modified electrodes

The SEM was used to observe the morphology of electrodes modified by different materials. As shown in Fig. 1A, it can be clearly seen that the MWCNTs modified glassy carbon electrode exhibited a highly entangled surface, and the relatively smooth morphology of MWCNTs can also be evidently observed, it showed that the

View Article Online
DOI: 10.1039/D0AY00025F

MWCNTs have excellent dispersion after acidification. We did not spray the electrode with gold due to the good electrical conductivity of MWCNTs. In addition, as illustrated in Fig. 1B, the crinkly GO can be clearly seen from the image of the poly-C DNA/GO/MWCNTs/GCE.

3.3 Electrochemical behaviors of the DNA biosensor

The measurements of CV and EIS were used for monitoring the electrochemical behaviors of the DNA biosensor. As illustrated in Fig. 2A, the peak current density of the bare GCE was smallest among that can be evidently observed (curve a). However, a significant enhancement has been captured after MWCNTs was modified onto the bare GCE (curve b). It was no doubt that the increase of current result from the excellent properties of MWCNTs, which including a large ratio of surface-to-volume and fast electron transfer. Subsequently, the peak currents of the electrode decreased in turn with the modification of poly-C DNA, BSA, and KAN (Fig. 2A, curve c, d, e). The results indicated the poly-C DNA and BSA were immobilized onto the electrode, and the aptamer captured the KAN. Modification of poly-C DNA and BSA on the electrode surface slowed the electron transfer rate, and the complex of the KAN-aptamer hinder the electron transfer, causing a decrease in current signal. In addition, the fabrication process of the DNA biosensor was further characterized by EIS method. In the Nyquist impedance plot, the fact that the semicircle represents the resistance of charge transfer (Rct) was well known.[37] As shown in Fig. 2B, apparently, the semicircle of the bare GCE (Rct= 314.2 Ω) was biggest compared with other modified electrodes, the value of Rct decreased much more than the bare GCE after

the modification of the MWCNTs, which was 15.62 Ω. It's caused by the fact that the conductive MWCNTs increased the electron transfer rate.[38] In addition, it was predictably that the value of Rct (31.60 Ω, curve c) was increased as the poly-C DNA/GO adsorption complex was immobilized onto the MWCNTs/GCE because the adsorption complexes block the electron transfer. In like manner, the Rct of the BSA/Poly-C DNA/GO/MWCNTs/GCE (36.80 Ω, curve d) increased again because the electrode was further modified by BSA. While incubated in 500 pM of KAN standard for 40 minutes, the Rct increased (43.10 Ω, curve e) due to the binding of aptamer of KAN and target. In detail, the corresponding electrochemical parameters from CV and EIS were listed in Table 1.

Table 1 Electrochemical parameters of different modified electrodes extracted from CV and EIS.

Electrode	Ipc (μA)	Ipa (μA)	Rs (Ω)	Rct (Ω)
GCE	41.98	-31.57	6.42	314.2
MWCNTs/GCE	150.5	-119.7	4.16	15.62
Poly-C DNA/GO/MWCNTs/GCE	126.1	-82.87	5.19	31.60
BSA/Poly-C DNA/GO/MWCNTs/GCE	106.3	-71.88	5.79	36.80
KAN/BSA/Poly-C DNA/GO/MWCNTs/GCE	92.48	-62.88	7.34	43.1

3.4 The optimizations of experimental parameters

In view of the influences of incubated time and pH on the DNA biosensor, we have optimized experiments for incubated time and pH. Firstly, we have performed the DPV electrochemical detection on the DNA biosensor under different incubation time. As illustrated in Fig. 3A, the DPV peak current density increased with the incubation time, and it reached a maximum at 40 min. When the incubation time was more than

View Article Online
DOI: 10.1039/D0AY00025F

40 min, the current density tends to be stable or decreased slightly. This means that the binding between the KAN and aptamer reached saturation at 40 min. In consequence, 40 min was seen as the optimal incubation time. In order to optimize the pH suitable for detection, the designed DNA biosensor has been performed detection in various pH of PBS (0.2 M) solution containing 5.0 mM $[Fe(CN)_6]^{3-/4-}$ and 0.1 M KCl. As shown in Fig. 3B, it can be clearly seen that the DPV peak current density was the largest when the pH was 7.4. However, when the pH was greater than 7.4, the current response signal gradually decreased due to the effect of high pH on bioactivity of diblock DNA with poly-cytosine. From the results, it indicated that the electrochemical sensing was best at pH 7.4.

Meanwhile, the pH during physical adsorption and the poly-C DNA concentration are also the critical factors affecting the efficiency of the DNA biosensor. Therefore, we made corresponding optimization experiments. As shown in Fig. S1(A), when the physical adsorption of poly-C DNA was carried out in HEPES buffer solutions of different pH, we can apparently see that when the pH is 7.5, the corresponding electrochemical signal value is the largest. As a result, it indicated that 7.5 is the optimal pH for the adsorption process. In addition, the optimization of poly-C DNA concentration during the physical adsorption is shown in Fig. S1(B), it can be observed that as the concentration of poly-C DNA increased, the current signal gradually increased and reached the maximum when the concentration is 10 μM. However, the electrochemical signal decreased after the concentration further increased. It's caused by the fact that an excess of poly-C DNA impeded the electron

View Article Online
DOI: 10.1039/D0AY00025F

transfer, reducing the electrochemical signal. As a consequence, 10 μM is the optimal adsorption concentration.

3.5 The detection of KAN

The analytical performance of the DNA biosensor was evaluated by detecting KAN in the PBS (0.2 M) solution under the optimal experiment conditions. We know that the specific binding of aptamer and target KAN would give rise to decrease of the DPV peak current density. As it is described, the Fig. 4A exhibited that the DPV peak current density decreased with the gradually increase of KAN concentration because of specific hybridization of target KAN with aptamer, which can be obviously seen also in Fig. S2. In the range of 0.05 pM-100 nM, an excellent linear correlation (R^2=0.997) has been displayed between the DPV peak current density (I(μA)) and logarithm values of the KAN concentrations (Fig. 4B). The regression equation was as follows, I(μA) = -121.2+3.089lg$C_{[KAN]}$ (pM), and the measured limit of detection (LOD) was 0.0476 pM (S/N=3). As listed in Table 2, we compared our works with the following results,[39-47] the detection limit and linear range were evidently better than the previous methods. In addition, it was worth mentioning that our method was very simple and reduced the damage to the activity of capture aptamer to a minimum compared with other complex techniques which require various markers.

View Article Online
DOI: 10.1039/D0AY00025F

Table 2 The work compared with other techniques for the detection of KAN.

Methods	Linear range	Limit of detection	Reference
Electrochemical aptasensor	0.0005-50 nM	0.15 pM	39
Electrochemical aptasensor	0.001-0.5 ng mL^{-1}	0.21 pg mL^{-1}	40
Electrochemical aptasensor	0.01-150 μg L^{-1}	0.005 μg L^{-1}	41
Potentiometric enzymatic aptasensor	0.05-30 pM	0.05 pM	42
Electrochemical aptasensor	0.1-4000 nM	35.69 pM	43
Imprinted electrochemical sensor	0.1-1000 nM	0.023 nM	44
Gas pressure-based bioassay	0.2-50 pM	0.063 pM	45
Photoelectrochemical aptasensor	1-230 nM	0.2 nM	46
Electrochemical DNA biosensor	0.05 pM-100 nM	0.0476 pM	This work

3.6 The specificity, reproducibility and stability of the DNA biosensor

The specificity was evaluated as one of the important parameters to demonstrate the performance of the DNA biosensor. AMX, CAP, STR, and OTC were selected as interferents to verify the specificity, and the concentrations of interferents approximately were 100 times of the KAN. As the results, as shown in Fig. 5, what we can clearly see was that the response of the DNA biosensor to the target KAN was the largest. On the contrary, the change of DPV electrochemical signal (ΔI(μA)) of the developed DNA biosensor for other interferent was so small that it can be almost ignored. As a result, we were safely arrived at the conclusion that the specificity of the designed DNA biosensor was excellent.

The reproducibility and repeatability of the DNA biosensor were also evaluated in PBS (0.2 M) solution containing 5.0 mM $[Fe(CN)_6]^{3-/4-}$ and 0.1 M KCl. Firstly, five

View Article Online
DOI: 10.1039/D0AY00025F

fresh DNA biosensors were prepared at the same time and they were used for the detection of KAN (500 pM). The relative standard deviation (RSD) was calculated to be 4.51%. And then we evaluated the repeatability by using a new prepared DNA biosensor repeatedly detected 500 pM of KAN for six times, the results indicated a small RSD of about 1.18%. Taking what has been discussed into consideration, it's indisputable that the DNA biosensors have both excellent reproducibility and repeatability.

Similarly, the stability of the DNA biosensor was also investigated in detail. After the new prepared DNA biosensor was stored at 4℃ for over 10 days, the change of DPV peak current density was tiny and only decreased about 8%. As illustrated in Fig. S3, the CV characterization was used for further verifying the stability of the DNA biosensor by measuring 50 cycles in the PBS (0.2M, pH=7.4) solution containing 5.0 mM $[Fe(CN)_6]^{3-/4-}$ and 0.1 M KCl. Ultimately, the peak current value of CV measurement can reach 94.6% of the initial current value. In consequence, the stability of the DNA biosensor was satisfactory.

3.7 Detection of KAN in milk samples

To study the performance of practical application of the designed DNA biosensor, it was used for detecting the KAN in milk samples. To begin with, the milk sample was centrifuged for 15 min under 10,000 rpm to remove possible distractions. Next, the sample was filtrated by polytetrafluoroethylene microfiltration membrane (0.22 μm) and was diluted 10 times with PBS (0.01M, pH=7.4). Then the 50 pM of KAN standard was spiked into milk samples. As shown in Table 3, the DNA biosensor has

View Article Online
DOI: 10.1039/D0AY00025F

high recovery distributions from 104.66% to 118.20%. From the results, it was enough to prove that the DNA biosensor has outstanding practical application in real samples.

Table 3 Analytical results for KAN in milk samples.

Samples	Added KAN (pM)	Detected (pM)	Recovery (%)	RSD (%, n=3)
Milk 1	50	52.33	104.66	9.44
Milk 2	50	53.64	107.28	9.11
Milk 3	50	59.10	118.20	6.08

4. Conclusions

In this study, an easily prepared electrochemical DNA biosensor based on the diblock DNA of 15-mer of poly-C was developed for sensitive, specific and efficient detection of KAN. The diblock DNA was designed as both fixed probe (adsorbing GO) and identified target without any marking. This biosensor was very easy to construct, and it avoided the problem of DNA activity damage that may be caused by DNA immobilization between the modified DNA and the substrate through covalent bonding. In addition, the DNA biosensor we designed has favorable specificity, stability, and practicality for testing in real samples. As a result, the presented DNA biosensor has wide linear range for KAN that was from 0.05 pM to 100 nM with the LOD of 0.0476 pM. Taking into account what we have discussed above, the electrochemical DNA biosensor is significantly potential suitable for the sensitive detection of other antibiotic residues in food.

View Article Online
DOI: 10.1039/D0AY00025F

Associated content

Supporting information

The DPV curves of the DNA biosensor toward different concentrations of KAN at the optimized conditions, the stability of the DNA biosensor.

Author information

Corresponding author

*Xiaoyan He

E-mail: hexy09@163.com

Tel: +86-13919132753

Author contributions

All authors have given approval to the final version of the manuscript.

Notes

The authors declare no competing financial interest.

Acknowledgements

This work was supported by the National Natural Science Foundation of China (NSFC) (No. 21765019, No. 21665024).

References

1. X. Bai, H. Hou, B. Zhang and J. Tang, *Biosens. Bioelectron.*, 2014, **56**, 112-116.
2. S. J. Wu, H. Zhang, Z. Shi, N. Duan, C. C. Fang, S. L. Dai and Z. P. Wang, *Food Control*, 2015, **50**, 597-604.
3. X. L. Qin, W. J. Guo, H. J. Yu, J. Zhao and M. S. Pei, *Anal. Methods*, 2015, **7**,

View Article Online
DOI: 10.1039/D0AY00025F

5419-5427.

4. C. A. Prosen, M. R. Petersen, D. B. Moody and W. C. Stebbins, *J. Acoust. Soc. Am*., 1978, **63**, 559-566.

5. W. Xu, Y. Wang, S. Liu, J. H. Yu, H. Z. Wang and J. D. Huang, *New J. Chem.*, 2014, **38**, 4931-4937.

6. J. K. Xue, J. Liu, C. S. Wang, Y. P. Tian and N. D. Zhou, *Anal. Methods*, 2016, **8**, 1981-1988.

7. L. Qin, G. M. Zeng, C. Lai, D. L. Huang, C. Zhang, P. Xu, T. J. Hu, X. G. Liu, M. Cheng, Y. Liu, L. Hu and Y. Y. Zhou, *Sens. Actuators B*, 2017, **43**, 946-954.

8. B. Li, X. Zhou, H. Liu, H. Deng, R. Huang and D. Xing, *ACS Appl. Mater. Interfaces*, 2018, **10**, 4494-4501.

9. R. Ren, G. Cai, Z. Yu and D. Tang, *Sens. Actuators B*, 2018, **265**, 174-181.

10. C. A. Toloza, J. M. Almeida, S. Khan, Y. G. Dos Santos, A. R. Da Silva, E. C. Romani, D. G. Larrudee, F. L. FreireJr and R. Q. Aucélio, *J. Pharm. Biomed. Anal*., 2018, **158**, 480-493.

11. Q. Wei, Y. F. Zhao, B. Du, D. Wu, H. Li and M. H. Yang, *Food Chemistry.*, 2012, **134**, 1601-1606.

12. G. Contreras Jiménez, S. Eissa, A. Ng, H. Alhadrami, M. Zourob and M. Siaj, *Anal. Chem.*, 2015, **87**, 1075-1082.

13. K. J. Huang, H. L. Shuai and J. Z. Zhang, *Biosens. Bioelectron*., 2016, **77**, 69-75.

14. D. S. Wilson and J. W. Szostak, *Annu. Rev. Biochem.*, 1999, **68**, 611-647.

15. S. Liu, Y. Wang, W. Xu, X. Q. Leng, H. Z. Wang, Y. N. Guo and J. D. Huang,

View Article Online
DOI: 10.1039/D0AY00025F

Biosens. Bioelectron., 2017, **88**, 181-187.

16. X. Chen, C. Y. Hong, Y. H. Lin, J. H. Chen, G. N. Chen and H. H. Yang, *Anal. Chem*., 2012, **84**, 8277-8283.
17. X. Qin, Y. Yin, H. Yu, W. Guo and M. Pei, *Biosens. Bioelectron*., 2016, **77**, 752-758.
18. P. J. J. Huang and J. Liu, *Anal. Chem*., 2012, **84**, 4192-4198.
19. K. Jayakumar, M. B. Camarada, V. Dharuman, R. Rajesh, R. Venkatesan, H. Ju, M. Maniraj, A. Rai, S. R. Barman and Y. Wen, *ACS Appl. Mater. Interfaces*, 2018, **10**, 21541-21555.
20. O. H. Laitinen, V. P. Hytönen, H. R. Nordlund and M. S. Kulomaa, *Cell. Mol. Life. Sci.*, 2006, **63**, 2992-3017.
21. Y. Hu, X. Xu, Q. Liu, L. Wang, Z. Lin and G. Chen, *Anal. Chem*., 2014, **86**, 8785-8790.
22. A. Miodek, N. Mejri, M. Gomgnimbou, C. Sola and H. Korri Youssoufi, *Anal. Chem*., 2015, **87**, 9257-9264.
23. T. M. Herne and M. J. Tarlov, *J. Am. Chem. Soc.*, 1997, **119**, 8916-8920.
24. Y. Chen, Y. Zhang, F. Pan, J. Liu, K. Wang, C. Zhang, S. Cheng, L. Lu, W. Zhang, Z. Zhang, X. Zhi, Q. Zhang, G. Alfranca, D. Chen and D. Cui, *ACS nano*, 2016, **10**, 8169-8179.
25. D. Cui, *J. Nanosci. Nanotechnol.*, 2007, **7**, 1298-1314.
26. A. Zhang, J. Chang, Y. Chen, Z. Huang, G. Alfranca, Q. Zhang and D. Cui, *Anal. Methods*, 2019, **11**, 5089-5097.

27. C. Lu, Z. Huang, B. Liu, Y. Liu, Y. Ying and J. Liu, *Angew. Chem. Int. Ed.*, 2017, **56**, 6208-6212.

28. Z. Huang and J. Liu, *Langmuir*, 2017, **34**, 1171-1177.

29. G. A. Rivas, M. D. Rubianes, M. C. Rodryguez, N. F. Ferreyra, G. L. Luque, M. L. Pedano, S. A. Miscoria and C. Parrado, *Talanta*, 2007, **74**, 291-307.

30. A. A. Ensafi, M. Amini and B. Rezaei, *Biosens. Bioelectron.*, 2014, **59**, 282-288.

31. M. Arvand, M. Sanayeei and S. Hemmati, *Biosens. Bioelectron.*, 2018, **102**, 70-79.

32. K. J. Chen, C. F. Lee, J. Rick, S. H. Wang, C. C. Liu and B. J. Hwang, *Biosens. Bioelectron.*, 2012, **33**, 75-81.

33. S. N. Kim, J. F. Rusling and F. Papadimitrakopoulos, *Adv. Mater.*, 2007, **19**, 3214-3228.

34. W. Zhou, J. Vavro, C. Guthy, K. I. Winey, J. E. Fischer, L. M. Ericson, S. Ramesh, R. Saini, V. A. Davis, C. Kittrell, M. Pasquali, R. H. Hauge and R. E. Smalley, *J. Appl. Phys.*, 2004, **95**, 649-655.

35. Y. D. Xue, S. L. Zheng, Z. Sun, Y. Zhang and W. Jin, *Chemosphere*, 2017, **183**, 156-163.

36. F. Rohrbach, H. Karadeniz, A. Erdem, M. Famulok and G. Mayer, *Anal. Biochem.*, 2012, **421**, 454-459.

37. N. Hui, X. Sun, S. Niu and X. Luo, *ACS Appl. Mater. Interfaces*, 2017, **9**, 2914-2923.

38. F. Li, Y. Guo, X. Wang and X. Sun, *Biosens. Bioelectron.*, 2018, **115**, 7-13.

39. M. Chen, N. Gan, Y. Zhou, T. H. Li, Q. Xu, Y. T. Cao and Y. J. Chen, *Talanta*,

View Article Online
DOI: 10.1039/D0AY00025F

2016, **161**, 867-874.

40. Z. H. Zhang, F. H. Duan, J. Y. Tian, J. Y. He, L. Y. Yang, H. Zhao, S. Zhang, C. S. Liu, L. H. He, M. Chen, D. M. Chen and M. Du, *ACS Sens*., 2017, **2**, 982-989.

41. H. Y. Song, T. F. Kang, N. N. Li, L. P. Lu and S. Y. Cheng, *Anal. Methods*, 2016, **8**, 3366-3372.

42. Y. Yao, C. Jiang and J. Ping, *Biosens. Bioelectron*., 2019, **123**, 178-184.

43. F. L. Li, X. Y. Wang, X. Sun, Y. M. Guo and W. P. Zhao, *Anal. Chim. Acta*, 2018, **1033**, 185-192.

44. F. Long, Z. H. Zhang, Z. X. Yang, J. H. Zeng and Y. Q. Jiang, *J. Electroanal. Chem*., 2015, **755**, 7-14.

45. R. Zeng, Z. Luo, L. Zhang and D. Tang, *Anal. Chem*., 2018, **90**, 12299-12306.

46. R. Li, Y. Liu, L. Cheng, C. Yang and J. Zhang, *Anal. Chem*., 2014, **86**, 9372-9375.

47. Y. Xie, X. Zhi, H. Su, K. Wang, Z. Yan, N. He, J. Zhang, D. Chen and D. Cui, *Nanoscale Research Letters*, 2015, **10**, 477.

View Article Online
DOI: 10.1039/D0AY00025F

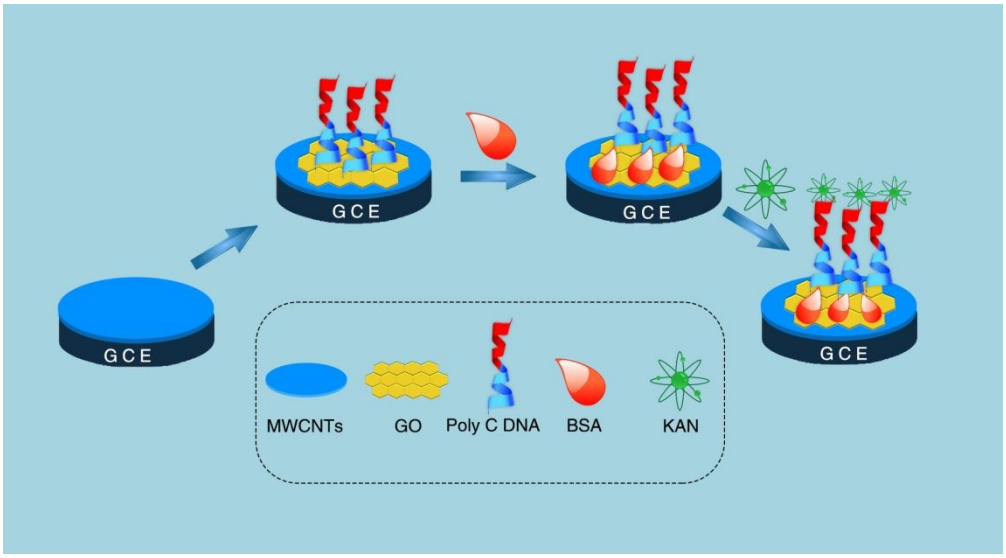

Scheme 1. Schematic illustration of fabrication process for the DNA biosensor.

View Article Online
DOI: 10.1039/D0AY00025F

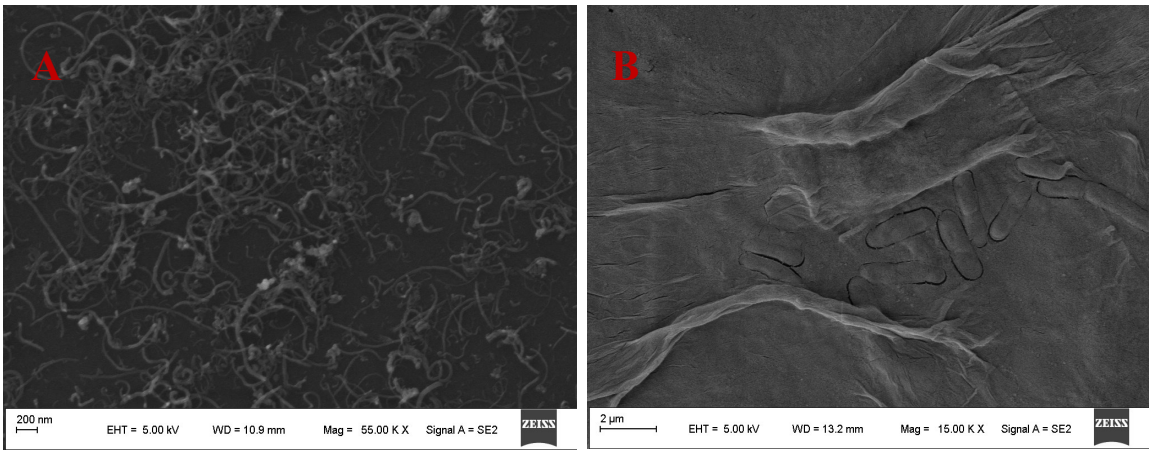

Fig. 1. SEM images of (A) MWCNTs/GCE and (B) poly-C DNA/GO/MWCNTs/GCE.

View Article Online
DOI: 10.1039/D0AY00025F

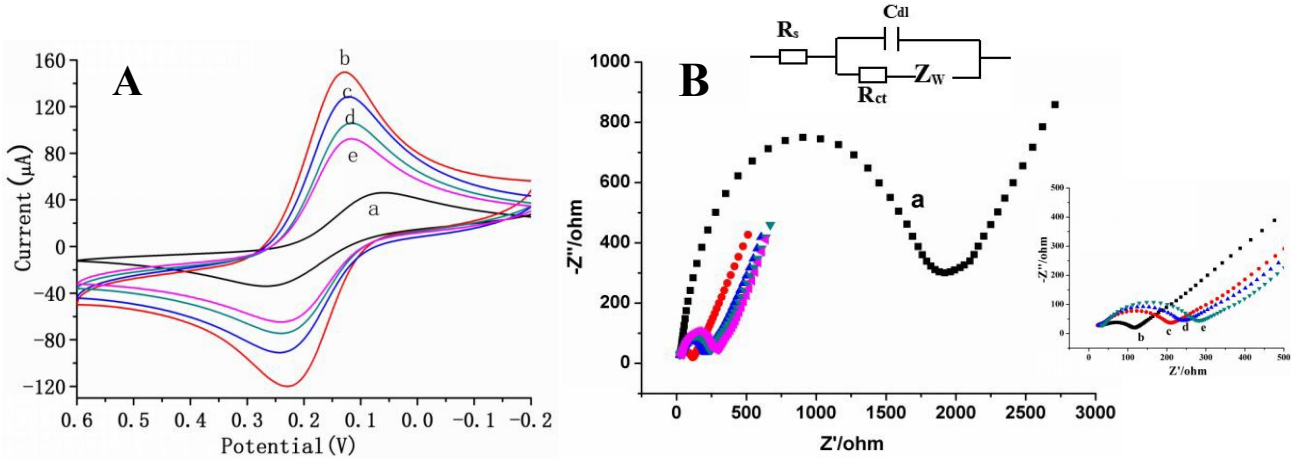

Fig. 2. CV (A) and EIS (B) responses measured in PBS (0.2 M, pH=7.4) solution containing 5.0 mM $[Fe(CN)_6]^{3-/4-}$ and 0.1 M KCl. The GCE (a); MWCNTs/GCE (b); Poly-C DNA/GO/MWCNTs/GCE (c); BSA/Poly-C DNA/GO/MWCNTs/GCE (d); KAN/BSA/Poly-C DNA/GO/MWCNTs/GCE (e). CV parameters: scanning range from -0.2 V to 0.6 V, and the scan rate was 0.05 V/s. EIS parameters: frequency range from 0.1 to 100 00 Hz with amplitude of the applied sine at 5 mV, and current potential of 0.162 V.

View Article Online
DOI: 10.1039/D0AY00025F

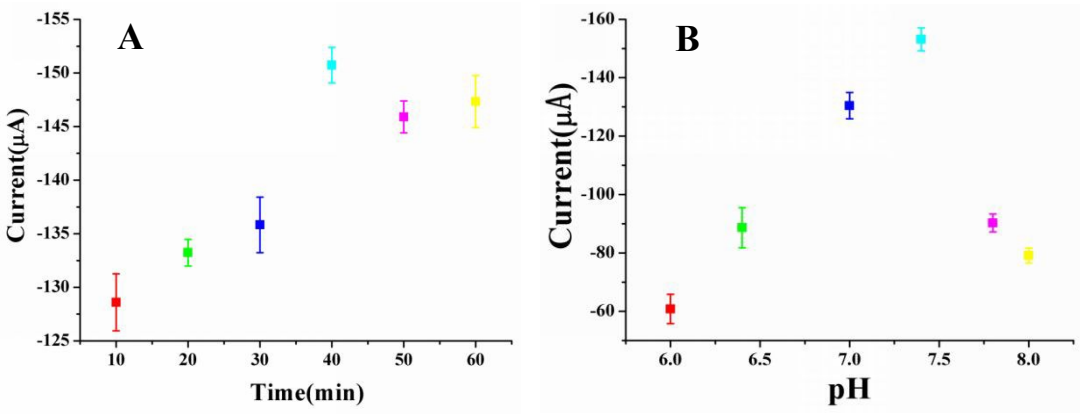

Fig. 3. The influences of incubation time (A) and pH (B) on the electrochemical DNA biosensor.

View Article Online
DOI: 10.1039/D0AY00025F

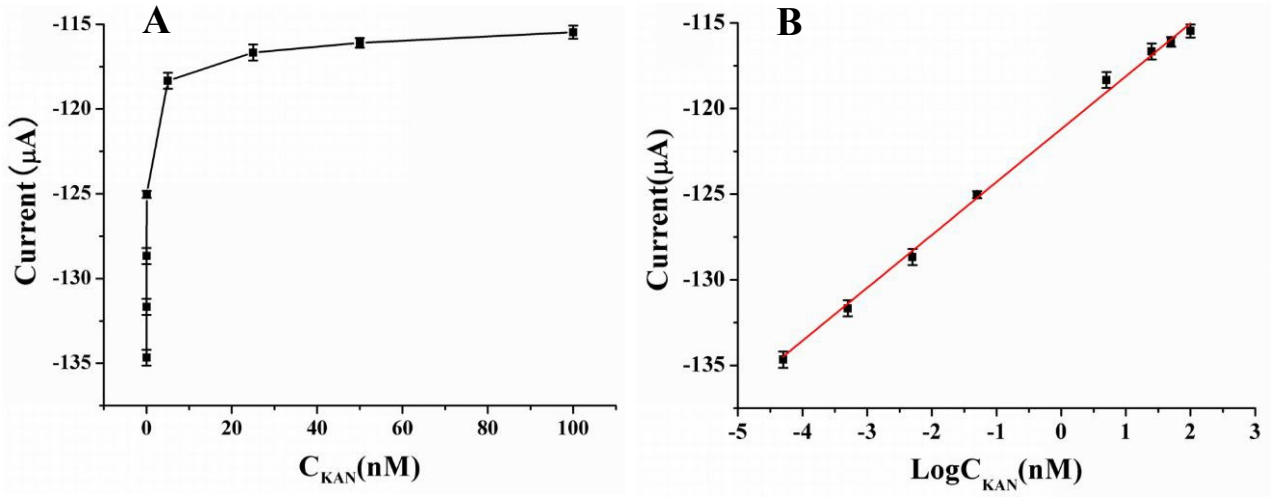

Fig. 4. (A) DPV peak current change of the DNA biosensor after incubation with different concentrations of KAN. (B) Calibration curve of KAN for different KAN concentrations from 0.05 pM to 100 nM.

View Article Online
DOI: 10.1039/D0AY00025F

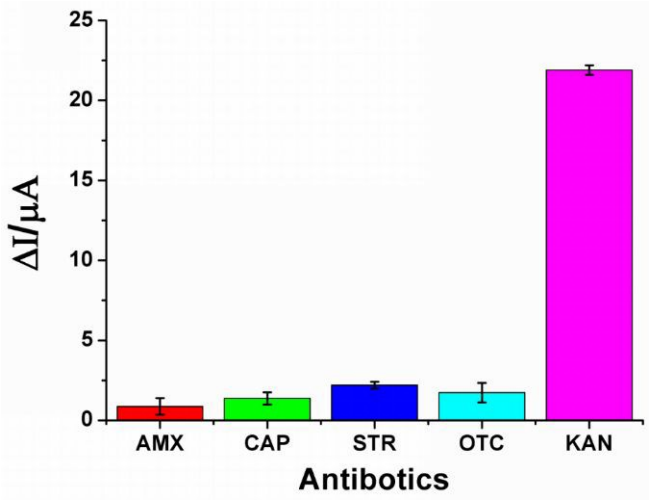

Fig. 5. Responses of the DNA biosensor to 2 μg/mL AMX, 2 μg/mL CAP, 2 μg/mL STR, 2 μg/mL OTC, and 500 pM KAN. The error bars represent the standard deviation of three repeated measurements.